Corrigendum to:

Optimization of bio-based cellulose–phosphate hydrogel production from rice husk waste using the Taguchi method

Selvia Aprilyanti[1*], Irnanda Pratiwi[1], Winny Andalia[1], Tine Aprianti[2,3], Hariman Al Faritzie[4]

Published in
Teknomekanik, Vol. 9, No. 1, February 2026, pp. 77–90

Original Article DOI
https://doi.org/10.24036/teknomekanik.v9i1.47172

Corrigendum DOI
https://doi.org/10.24036/teknomekanik.v9i3.59372

Editorial Note

This Corrigendum was submitted by the corresponding author on behalf of all co-authors and has undergone editorial assessment in accordance with Teknomekanik's Post-Publication Corrections Policy. After careful evaluation, the Editorial Board determined that the proposed corrections are limited to presentation accuracy and consistency, including figure replacement, figure captions, textual clarification, and integration of the related discussion. The Editorial Board confirms that these corrections do not affect the research methodology, experimental data, statistical analyses, scientific findings, interpretation, or conclusions of the original article. Accordingly, this Corrigendum has been approved for publication.

Author Statement

The authors regret that several presentation errors were identified after publication. The corrected figures and associated text are provided in this Corrigendum. These corrections do not affect the scientific results or conclusions of the original article. The authors apologize for any inconvenience caused.

Reason for Correction

Following publication of the above article, the authors identified several presentation inconsistencies involving Figures 3–7 and the associated narrative descriptions.

The corrections include:

1. replacement of Figure 3 with a schematic consistent with the phosphoric-acid-assisted phosphorylation mechanism;
2. improved integration of Figures 3 and 4 within the methodology section;
3. correction of the interpretation associated with Figure 5;
4. clarification of the FTIR discussion related to Figure 6;
5. correction of the SEM magnification in Figure 7 from 5× to 5,000×;
6. improved consistency between figure captions, graphical content, and the corresponding scientific discussion.

These corrections are intended solely to improve the accuracy and clarity of presentation.

Summary of Corrections

No	Section	Type of Correction
1	Figure 3	Figure replacement, caption revision, and associated text revision
2	Figure 4	Additional narrative description and explicit reference to Figure 4
3	Figure 5	Caption and discussion revised
4	Figure 6	Discussion revision and explicit reference to Figure 6
5	Figure 7	Caption corrected and discussion expanded

Correction 1 – Figure 3

Section: 2.5 Bio-based absorbent hydrogel synthesis process
Location: Page 81, Figure 3
Type of Correction: Figure replacement, caption revision, and associated text revision

Original version

The original Figure 3 illustrated a bio-based double crosslinked cellulose hydrogel system involving epoxidized vegetable oils as the crosslinking mechanism. The accompanying text also described chemical crosslinking between cellulose hydroxyl groups and epoxidized vegetable oils. This illustration and description were inconsistent with the actual experimental procedure reported in the study.

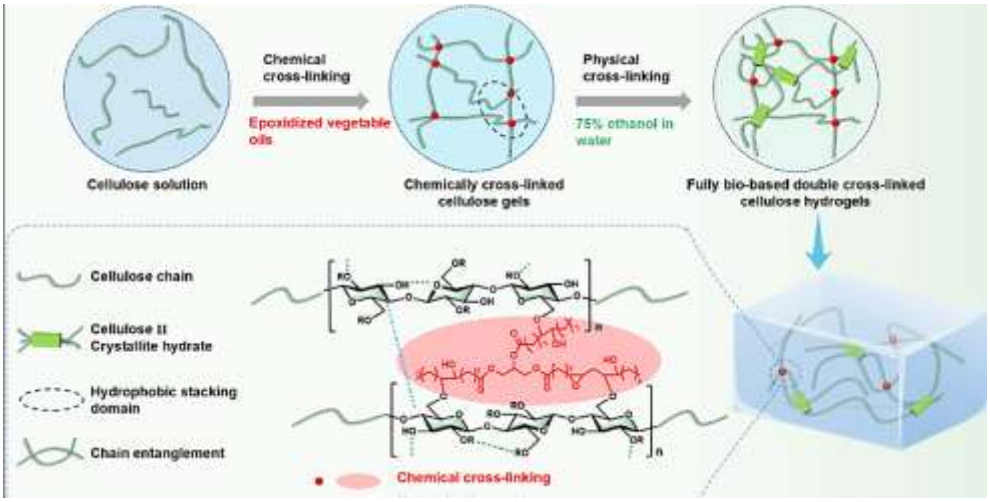

Figure 3. Schematic illustration of a bio-based double crosslinked cellulose hydrogel system

Corrected version

Before crosslinking, the extracted rice husk cellulose was dispersed in 30 mL of distilled water and allowed to hydrate for 24 h. Phosphoric acid was subsequently added according to the experimental conditions specified in the Taguchi design. The proposed formation mechanism of the cellulose–phosphate hydrogel is illustrated in Figure 3.

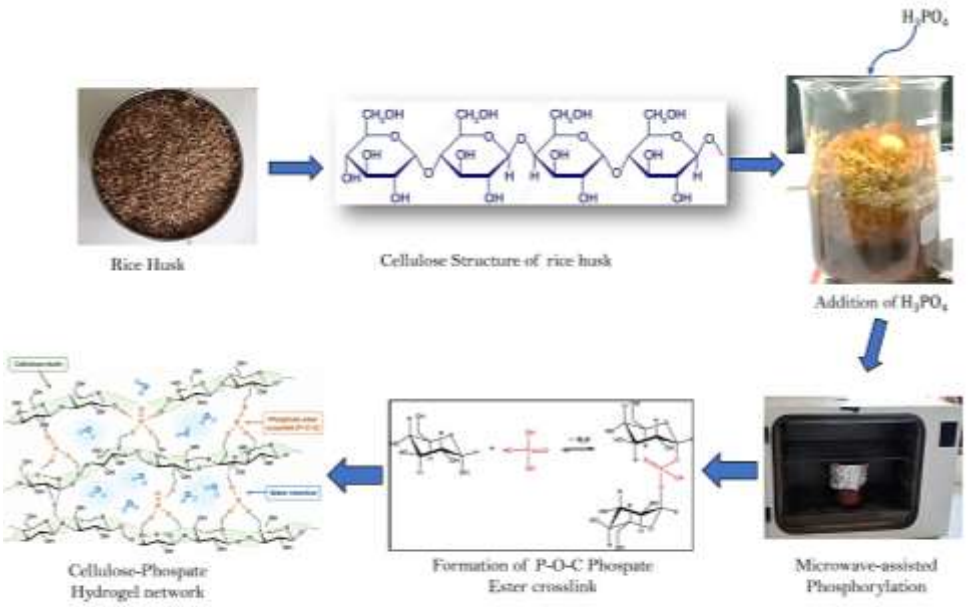

Figure 3. Schematic representation of phosphate crosslinking in rice husk cellulose hydrogel

As shown in Figure 3, the crosslinking process involves the interaction of phosphoric acid with hydroxyl groups present on the cellulose chains, leading to the formation of phosphate ester linkages and a chemically cross-linked cellulose gel [29]. The mixture was subjected to microwave-assisted heating at a fixed power output, while reaction time and temperature were varied based on the Taguchi orthogonal array [30]. Under controlled microwave-assisted heating, phosphorylation promotes the formation of phosphate ester linkages, particularly P–O–C bonds, between cellulose chains. These chemical linkages contribute to the development of a three-dimensional hydrophilic network capable of absorbing and retaining water. The proposed mechanism is consistent with the phosphate-related functional groups subsequently identified by FTIR analysis.

Correction 2 – Figure 4

Section: 2.5 Bio-based Absorbent Hydrogel Synthesis Process
Location: Page 81, Figure 4
Type of Correction: Additional narrative description and explicit reference to Figure 4

Original version

After completion of the reaction, the mixture was cooled to room temperature, filtered, and repeatedly washed with distilled water to remove unreacted species. The resulting hydrogel was dried to constant weight and stored for further characterization.

(Figure 4 was presented without explicit discussion in the accompanying text.)

Corrected version

Following the crosslinking reaction, the mixture was cooled to room temperature, filtered, and repeatedly washed with distilled water to remove residual phosphoric acid and other unreacted species. The resulting hydrogel was subsequently dried to constant weight before further characterization. The complete sequence of the cellulose–phosphate hydrogel synthesis procedure is summarized in Figure 4.

As illustrated in Figure 4, the synthesis procedure consisted of five principal stages: (1) dispersion and hydration of extracted rice husk cellulose in distilled water, (2) addition of phosphoric acid followed by microwave-assisted heating under the experimental conditions specified by the Taguchi design, (3) filtration of the reacted mixture, (4) repeated washing with distilled water to remove residual reactants, and (5) drying of the resulting cellulose–phosphate hydrogel. This sequential procedure ensured that the samples used for swelling, FTIR, and SEM characterization were prepared under consistent experimental conditions.

Correction 3 – Figure 5

Section: 3.2 Signal-to-Noise Ratio (SNR)
Location: page 84
Type of Correction: Caption and discussion revised

Original version

Figure 5. Means response graph for each parameter level

The main effects plot of SNR values revealed that phosphoric acid volume exerted the strongest influence on swelling performance, followed by cellulose content and heating temperature. Reaction time showed a comparatively smaller effect. These trends suggest that the extent of crosslinking and the availability of hydrophilic functional groups play a critical role in governing water absorption behavior.

Corrected version

Figure 5. Main-effects plots of mean swelling ratio

As shown in Figure 5, cellulose content exhibited the largest variation in the mean swelling ratio across the investigated factor levels. The swelling response increased slightly as the cellulose content increased from 1 to 3 g, followed by a pronounced decrease at 4 g. This trend suggests that excessive cellulose content may increase network density and restrict the expansion of the hydrogel matrix, thereby reducing water uptake. Phosphoric acid volume also influenced swelling performance, with the highest average swelling response observed at an intermediate acid volume rather than at the highest level. This behavior indicates that an optimum degree of phosphorylation is required: insufficient crosslinking may produce a weak network, whereas excessive crosslinking may restrict polymer-chain mobility and reduce the available free volume for water absorption. Reaction time and heating temperature produced comparatively smaller variations in mean swelling response. Overall, the trends presented in Figure 5 are consistent with the ANOVA results in Table 5, which identify cellulose content as the dominant statistically significant factor affecting swelling performance.

Correction 4 – Figure 6

Section: 3.4 FTIR Analysis
Location: Page 85, Figure 6
Type of Correction: Discussion revision and explicit reference to Figure 6

Original version

Fourier Transform Infrared Spectroscopy (FTIR) was used to investigate chemical interactions and confirm crosslinking between rice husk cellulose and phosphoric acid. The FTIR spectrum of raw cellulose exhibited a broad absorption band at approximately 3340–3400 cm^{-1} corresponding to O-H stretching vibrations, as well as a characteristic peak near 1050 cm^{-1} associated with C-O stretching of the cellulose backbone.

Following crosslinking, notable spectral changes were observed in the hydrogel. The intensity of the O-H stretching band decreased and broadened, indicating the involvement of hydroxyl groups in esterification reactions. In addition, new absorption bands appeared in the regions of 1240–1260 cm^{-1} and 1020–1080 cm^{-1}, which are characteristic of P=O stretching and P-O-C asymmetric stretching vibrations, respectively. The emergence of these phosphate-related bands provides clear evidence of phosphate ester bond formation between cellulose chains. These findings confirm successful crosslinking and the formation of a chemically stable cellulose–phosphate network, consistent with previously reported phosphate-crosslinked cellulose hydrogels.

Corrected version

Fourier Transform Infrared Spectroscopy (FTIR) was used to investigate chemical interactions and confirm crosslinking between rice husk cellulose and phosphoric acid. The comparative FTIR spectra of the cellulose precursor and the resulting cellulose–phosphate hydrogel are presented in Figure 6.

As shown in Figure 6, the cellulose-based samples exhibited a broad absorption region around 3310–3400 cm^{-1} associated with O–H stretching vibrations. Changes in the intensity and position of this band after hydrogel formation indicate modification of the hydrogen-bonding environment and participation of cellulose hydroxyl groups during the crosslinking process. The phosphate-crosslinked hydrogel also exhibited characteristic absorption features in the region around 1245 cm^{-1} and approximately 1045 cm^{-1}, which were assigned to phosphate-related stretching vibrations, including P=O and P–O–C functionalities. The presence and modification of these bands support the formation of phosphate-containing linkages in the hydrogel network. Therefore, the spectral features shown in Figure 6 provide chemical evidence supporting the proposed cellulose–phosphate crosslinking mechanism illustrated in Figure 3.

Correction 5 – Figure 7

Section: 3.5 SEM morphological analysis
Location: Page 86, Figure 7
Type of Correction: Caption correction and discussion enhancement

Original version

Figure 7. SEM micrograph of cellulose hydrogel at 5x magnification

Scanning Electron Microscopy (SEM) was employed to examine the surface morphology and pore structure of the cellulose-phosphate hydrogel synthesized under optimal conditions. The SEM micrographs revealed a porous, non-uniform surface architecture with an interconnected network.

Based on the scale bar and visual estimation, pore diameters ranged approximately from 2.0 to 6.5 μm, with the majority distributed in the 3–5 μm range. This porous morphology facilitates capillary-driven water diffusion and enhances swelling capacity by allowing efficient penetration of water molecules into the hydrogel matrix. The interconnected pore structure indicates effective phosphate ester crosslinking, which forms a three-dimensional network while preventing excessive chain packing. This morphological characteristic is consistent with the experimentally observed swelling behavior and supports the formation of a stable absorbent hydrogel network.

Corrected version

Figure 7. SEM micrograph of cellulose–phosphate hydrogel at 5,000× magnification

Scanning Electron Microscopy (SEM) was employed to examine the surface morphology and pore structure of the cellulose–phosphate hydrogel synthesized under optimal conditions. The SEM micrographs revealed a porous and non-uniform surface architecture with an interconnected network structure. The representative SEM micrograph is presented in Figure 7.

As shown in Figure 7, the hydrogel exhibited a heterogeneous porous morphology characterized by interconnected cavities distributed throughout the polymer matrix. Based on the 5 μm scale bar, the visible pores were predominantly within the micrometer range, with noticeable variation in pore size and shape across the imaged surface. The pore walls appeared relatively thin and continuous, forming an irregular, sponge-like three-dimensional network.